Spatial Resolution Enhancement of Cassini Titan Radar Mapper Data

David G. Long

***Abstract*—Post processing reconstruction and resolution enhancement algorithms can be applied to Cassini Titan Radar Mapper data to improve the image resolution for scatterometer-mode imagery. Reconstruction algorithms can also yield enhanced resolution images when multiple passes are combined. This paper briefly describes the application of the AVE and the Scatterometer Image Reconstruction (SIR) algorithms to Cassini Radar data. Some sample results are provided. A comparison with the Backus-Gilbert algorithm is also provided.**

I. Introduction

THE Cassini mission to Saturn includes a radar sensor to image the surface of the moon Titan, which has a thick, optically opaque atmosphere [1]. The Cassini Radar Mapper sensor can be operated in a low-resolution scatterometer mode or in a high resolution synthetic aperture radar (SAR) mode. Both operate by transmitting a pulse of microwave energy towards the surface and measuring the reflected energy. The backscattered energy is related to the normalized radar backscatter cross-section (NRCS) via the radar equation. The spatial response function of the sensor determines the spatial resolution of the observations. Using coherent processing of Doppler information, the SAR mode provides the highest resolution imagery. In contrast, SAR-type processing cannot be used with the scatterometer measurements [2]. This limits the effective resolution of the resulting scatterometer images.

Recent developments in radar reconstruction and resolution enhancement suggest that reconstruction algorithms can be used to improve the spatial resolution of scatterometer mode data in post-processing. They can also be of value in combining multiple pass data. In particular, the Scatterometer Image Reconstruction (SIR) technique can improve the effective spatial resolution of imagery collected with sufficient oversampling, especially when multiple measurements with diversity of spatial response functions are available [3].

In this paper, we consider the application of several reconstruction/resolution enhancement techniques to Cassini radar data. First, reconstruction theory is briefly described and the limitations of the theory as applied to SAR-processed Cassini data is considered. Then, the reconstruction algorithms are described and sample results presented. A comparison of SIR, AVE, and Backus-Gilbert algorithms are provided. The spectra of the measurements and images are considered. Finally, a brief conclusion is provided.

The author is with the Dept. of Electrical and Computer Engineering, Brigham Young University, 459 Clyde Building, Provo, UT 84602 USA (801-422-4383; long@ee.byu.edu).

II. Reconstruction Theory

The purpose of this paper is to evaluate the feasibility of using post-processing reconstruction/resolution enhancement techniques to Cassini radar data. The goal is to improve the effective resolution of the data to better interpret geological features. In conducting this study, we are trying to optimize image quality from data collected by an existing sensor not designed for application of the reconstruction algorithm.

Advanced reconstruction and resolution enhancement techniques such as the Scatterometer Image Reconstruction (SIR) and the Backus-Gilbert [7],[8] algorithms have proven to be very useful in improving the utility of scatterometer and radiometer data [3]–[6]. These signal processing techniques can be used to provide improved resolution measurements from microwave sensors. SIR been applied to scatterometers such as SeaWinds [3] as well as radiometers such as AMSRE and SMM/I [6]. SIR has also been studied for use with the proposed HYDROS, which includes a radiometer, scatterometer, and low resolution SAR [5].

The fundamental idea in the reconstruction is to take advantage of the high frequency information contained in oversampled measurements by reconstructing the aperture-filtered signal and inverting the spatial measurement response function (SRF) to estimate the radar backscatter (or brightness temperature in the case of radiometers) at higher spatial resolution. Since enhancing the resolution also enhances the noise, there is a tradeoff between resolution enhancement and noise [3],[6].

In conventional signal processing, reconstruction of uniformly spaced measurements is achieved by low-pass filtering zero-hold data. Assuming the Nyquist rate is met, the effective resolution of such processing is typically limited to the extent of the 3 dB response of the spatial response function. However, higher resolution can be obtained using full reconstruction theory, which, in effect, convolves the measurements by the inverse spatial response function, i.e. deconvolving the spatial response function, as part of the reconstruction. We note that uniform sampling is not required.

To be effective, reconstruction requires 1) oversampling of the signal, 2) a spatial response that has no nulls in its spectrum over the desired frequency range, and 3) sufficiently high SNR since the deconvolution tends to amplify high frequency noise. If these requirements are met, the signal can be reconstructed to higher resolution than the 3dB extent of the spatial response function. However, as noted, there is a tradeoff between reconstruction resolution and noise since the

978-1-4244-2871-7/09/$25.00 ©2009 IEEE

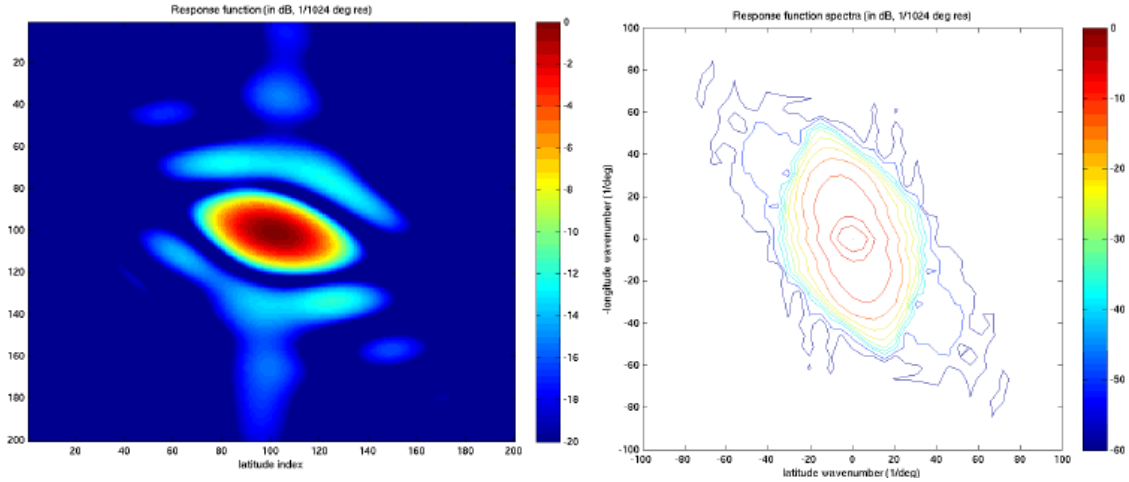

reconstruction tends to act as a high pass filter. Combining measurements with varying SRF is particularly effective [3].

In this paper two reconstruction algorithms based on the iterative scatterometer image reconstruction (SIR) algorithm [3], modified for single-variate reconstruction, are used. These are compared with another reconstruction techniques, the Backus-Gilbert algorithm. SIR and AVE have the advantage of not requiring uniform sampling and, compared to the Backus-Gilbert algorithm, require less computation [6].

Conventionally, the intrinsic resolution of the measurements

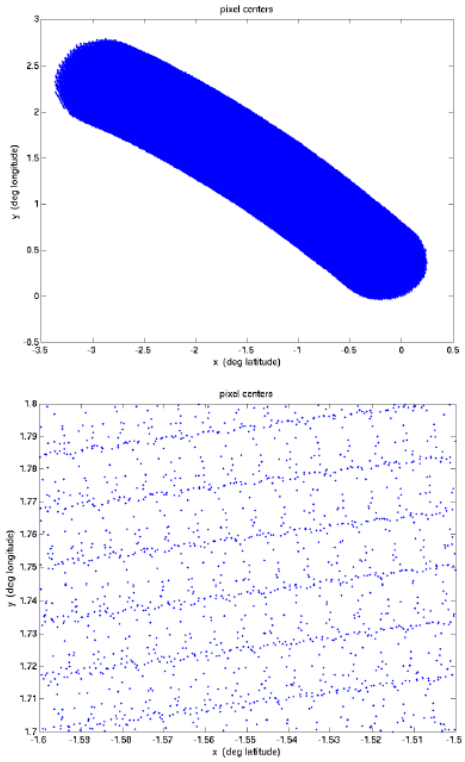

Fig. 2 Sampling locations for the pass of interest. (top) Locations for the full data take. (bottom) Zoom-in view showing density and irregular spacing of the observations.

is normally considered to be dictated by the 3 dB extent of the SRF on the surface. For SAR, this is the SRF of the processed image pixels. For scatterometers, the SRF is a function of the antenna pattern and onboard signal processing. Note that in general the SRF may be different for each measurement.

With sufficiently dense spatial sampling, the primary limitation to reconstruction is the SRF. The SRF acts as a spatial filter on the surface backscatter function that must be inverted as part of the reconstruction. In effect, the reconstruction takes advantage of sidelobes in the response function to recover higher frequency information. If, however, the gain of the response pattern at any given spatial frequency is too low, the signal cannot be recovered since any noise present in the measurements at that frequency is overly amplified in the inversion. A practical limitation to the recovery is a response function spectral gain more than 40-50 dB down from the peak, though this number is reduced when the measurement SNR is low [5]. Unfortunately, low SNR is common for the Titan Radar. For this paper the Titan Radar SRF is computed from a model of the Cassini antenna, the onboard signal processing, and the observation geometry.

III. Scatterometer Mode Reconstruction/Enhancement

We first consider the case of a single data collection mode with data obtain during a particular pass. Multiple passes are considered later. The data collection of interest has (essentially) a single, constant SRF. The measurements are collected on an irregular, dense grid. Fig. 1 illustrates the SRF and its 2-d spectrum for this data collection while Fig. 2 illustrates the sampling density of the measurements. We note that the elliptical shape of the SRF results in an elliptical spectrum that is not aligned with the imaging axis. We further note that the frequency response has a very sharp rolloff. Unfortunately, this fundamentally limits the performance of the reconstruction. (Sensors with higher sidelobes can achieve better reconstruction, see [3]). With no usable sidelobes Cassini Radar Mapper reconstruction and enhancement is limited to enhancement of spatial information within the main lobe of the frequency response. Thus, the expected resolution

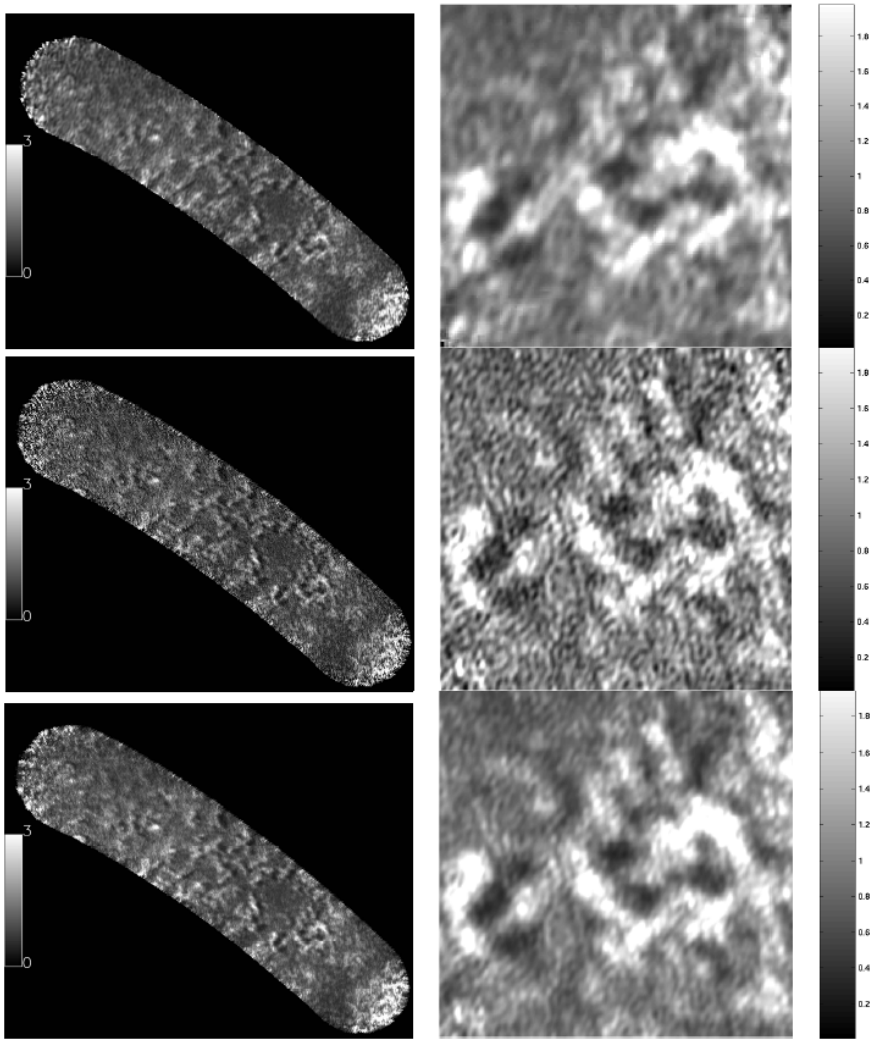

Fig. 3. Sample reconstruction results. (left column) full-coverage images. (right column) 1 deg by 1 deg sub images. (top row) conventional images. (center row) SIR algorithm. (bottom row) AVE algorithm.

improvement is limited.

In the following, reconstruction performance is shown for both the full SIR algorithm and the AVE algorithm. These are compared with the Backus-Gillbert algorithm. AVE is a very simple resolution enhancement algorithm, equivalent to the first iteration of SIR [4]. The SIR algorithm improves the effective spatial resolution from the initial AVE image estimate via iteration. It inverts both the sampling and SRF.

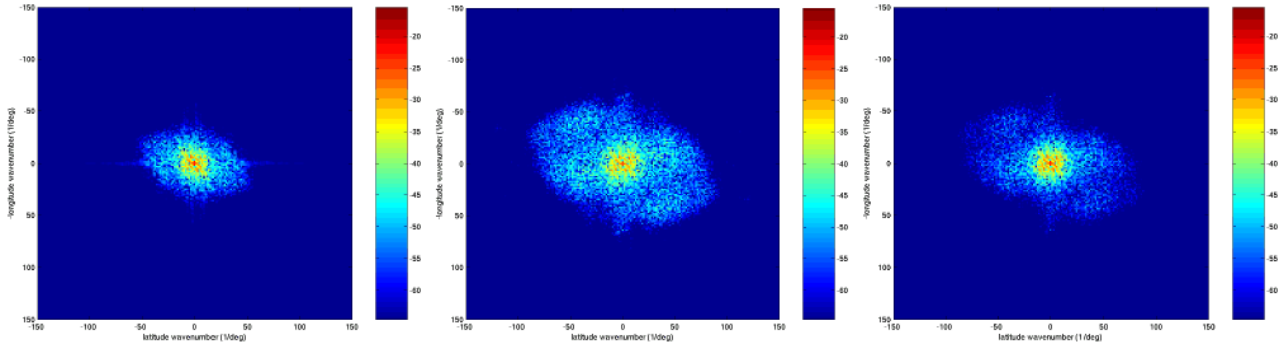

Fig. 4. Two-dimensional spectra of the images shown in Fig. 3. (left) Conventional. (center) SIR. (right) AVE. Note the additional spectral region of support contained in the SIR and AVE spectra compared to the conventional spectra.

The resolution/noise tradeoff is controlled by the number of iterations of SIR [3].

Figure 3 compares the conventionally computed image with images computed using AVE and SIR reconstruction. Note that both AVE and SIR offer resolution enhancement over the conventionally processed image, but at the expense of added noise. The AVE image has less resolution than SIR, but also has less noise. The SIR image has improved contrast, though higher noise. The improved resolution is confirmed by examining the wider image spectra shown in Figs. 4 and 5.

In order to simplify comparison the spectra of various cases, 1-d (row, column) average spectra are shown in Fig. 5. To compute these curves, the 1-d spectra of the rows and columns are computed and separately averaged. The row and column spectra differ due to the contents of the image. The spectra are normalized to the same DC value. Note that while there is a general rolloff in power versus frequency in the images, the conventional image spectra plots include large peaks at high frequencies near the Nyquist cutoff frequency. These peaks are artifacts resulting from spectral aliasing in the process of conventional image construction and do not represent useful information in the image. Note that the AVE and SIR images do not show this contamination.

We note that in Fig. 5 that the SIR image has greater energy

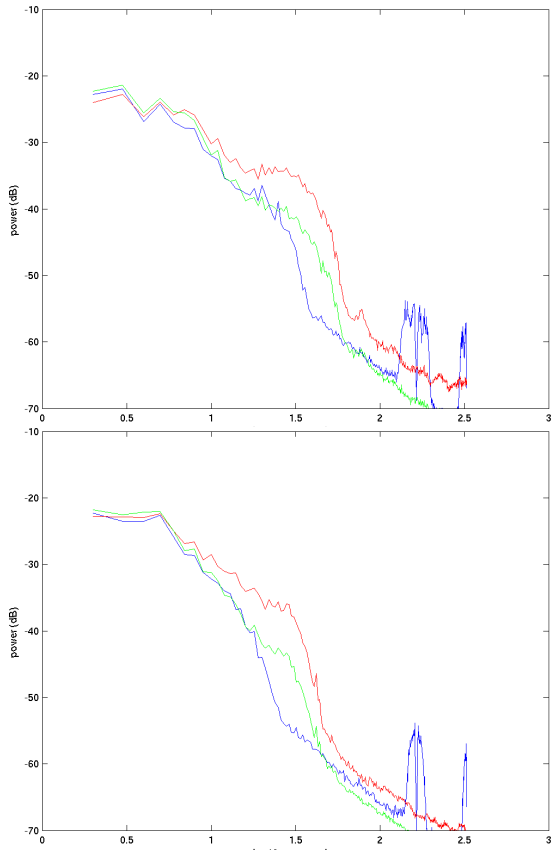

Fig. 5. Averaged 1-d spectra for (right) row and (left) columns of the images shown in Fig. 3. The blue line corresponds to the spectra of the conventional image, while red and green correspond to the SIR and AVE images, respectively.

at high frequencies compared to the conventional image and thus better contrast. However, we also note that the SIR image has a higher "noise floor" at the highest frequencies compared to AVE and the conventional image. This is the result of the enhancement of the noise intrinsic to the reconstruction.

IV. Comparison with Backus-Gilbert

The Backus-Gilbert (BG) technique is an alternate method of reconstruction that seeks to maximize the resolving power subject to stability and noise considerations [3,7]. It includes

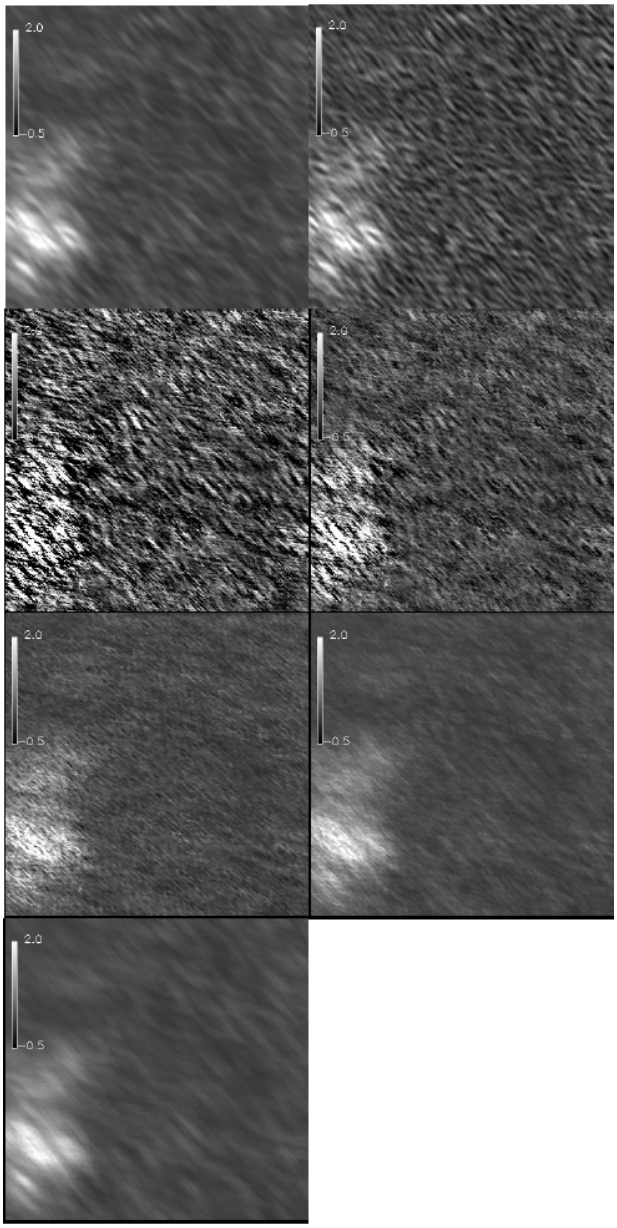

Fig. 6. Comparison of AVE, SIR, and BG for various values of the BG tuning parameter γ for an arbitrarily selected small region of T16. (top left) AVE. (top right) SIR at 100 iterations. (left to right, top to bottom) BG for various values of γ (0.495, 0.495,0.4995, 0.49995, 0.5)

a tuning parameter that must be subjectively chosen. The tuning parameter explicitly enables a tradeoff between noise and resolution. The BG technique is widely used in radiometry, but requires more computation than SIR [6].

We compare the reconstruction performance of BG compared to SIR and AVE. Due to the computational requirements of BG, the comparison is limited to a small area. Figure 6 compares SIR (100 iterations), AVE, and BG for various values of the BG tuning parameter γ. Comparison of the results shows that at γ=0.5 the BG image is similar to the AVE result.

V. Combined Passes

Combining overlapping SAR and scatterometer-mode observations from different passes can improve the effective resolution of the images, though the high noise level of the scatterometer-mode measurements remains a limitation. Due to the instrument characteristics, the SRFs of the two modes have somewhat different shapes. The reconstruction exploits this in the processing as suggested in [4],[5]. Figure 7 illustrates how the relative orientations of the SRFs improve the resolution of the Cassini T16 modes.

In the case of the two passes in the Cassini T16 dataset, the similiarities in the SRFs limit the improvement in effective resolution from averaging measurements since they are less different in aspect than desired [4]. Nevertheless, some improvement in the spatial resolution is observed in Fig. 7. In particular, the region of spectral space contained within the 3dB contour is larger for the averaged SRFs compared to the individual measurements. While the improvement is relatively small for the 3dB contour, it is more significant at lower contour levels. Note that full reconstruction does better than merely averaging the SRFs.

Figure 8 illustrates a small segment of the T16 data collection. Separate images of both collection schemes are shown. In addition, the averaged SRF image (labeled dual) is generated by averaging the other two images. Since the sampling grid for the two resolution modes is different, a pixel-by-pixel average is not possible. Instead, an AVE-like approach is used. Thus, the dual image has higher resolution than either mode separately. This is confirmed in the spectra of the images (not shown).

The SIR image with 100 iterations and a true AVE image is also shown in Fig. 8 for comparison. The AVE image has less resolution than the dual, but has less noise. The SIR image reveals some additional detail and has improved edges. However, the noise level is higher. This is not surprising since the SAR measurements contain speckle noise, which has high variance. Simulations verify the limited improvement possible with single look speckle noise.

VI. Conclusion

Full reconstruction algorithms are, in effect, inverting the SRF, i.e. applying a filter whose response corresponds to the inverse of the SRF spectra. We note that in the uniform

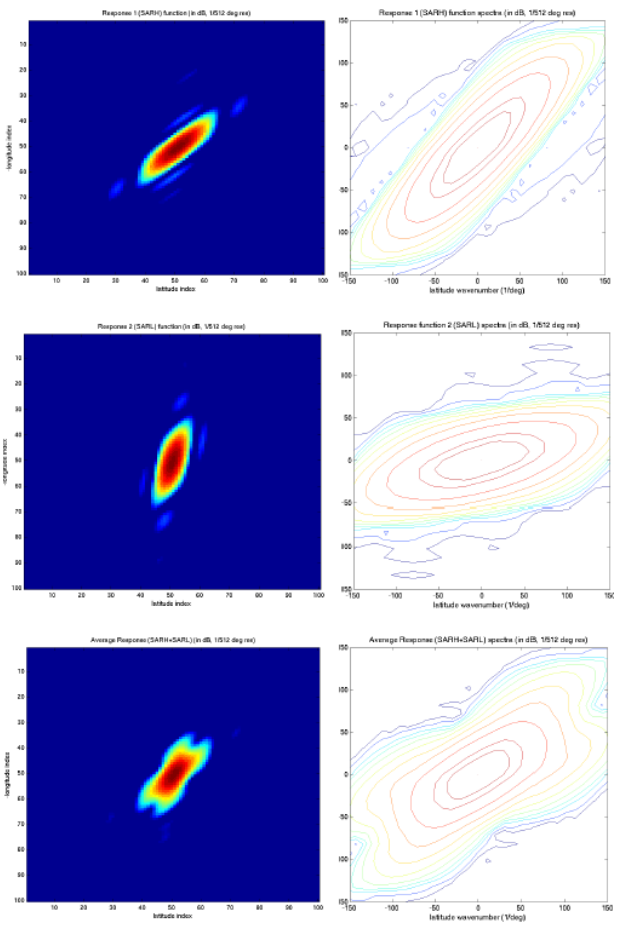

Fig. 7. Cassini T16 example SRFs (left column) and their spectra (right column). (top row) SARH. (center row) SARL. (bottom row) average of SRFs. Note that the averaged spectra covers a larger area.

sampling case, this could be equivalently done using a Weiner filter. However, the SIR and BG algorithm are capable of dealing with the irregular sampling fundamental to the data set. We note that the sidelobes in the Cassini Radar Mapper scatterometer mode SRF are very low, and thus unrecoverable with the relatively high noise level in the data. This limits the reconstruction resolution possible for this sensor. While the reconstructed imagery does have improved contrast and resolution, it is not clear if this provides additional information contributing to the interpretation of the imagery.

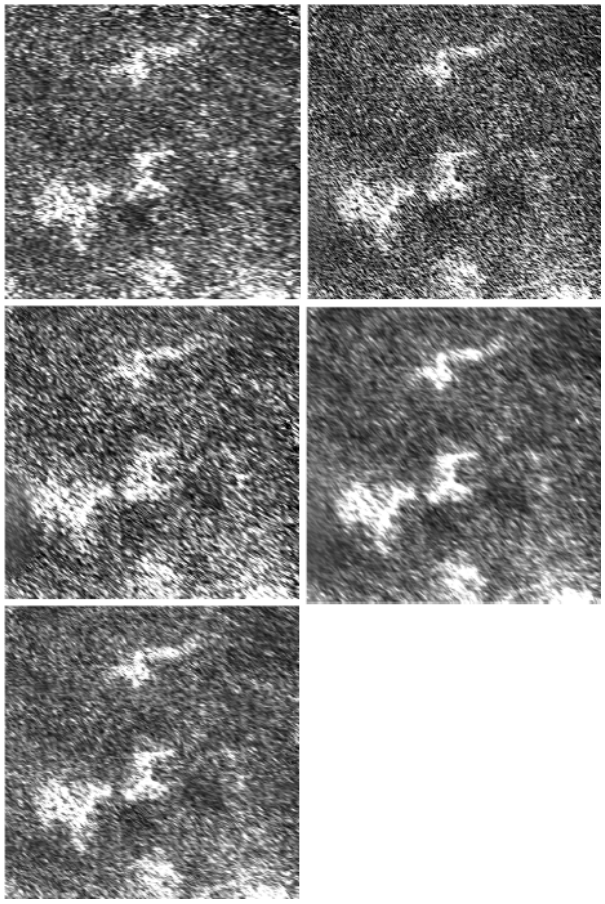

FIG. 8. T16 sub image results from a small (2 deg by 2 deg) area of Titan constructed from combined SARL and SARH measurements. (upper left) SARL image. (center left) SARH image. (lower left) Average of SARL and SARH using an AVE-type approach. (upper right) SIR with 100 iterations. (center right) AVE result using both SARL and SARH.

VII. ACKNOWLEDGEMENTS

The author thanks Bryan Stiles for providing Cassini Radar Mapper data and its SRF information.

REFERENCES

[1] C. Elachi, E. Im, L.E. Roth, and C.L. Werner, "Cassini Titan Radar Mapper," *Proc. IEEE*. Vol. 79, no. 6, pp. 867-880, 1991

[2] http://saturn.jpl.nasa.gov/spacecraft/instruments-cassini-radar.cfm

[3] D.S. Early and D.G. Long, "Image Reconstruction and Enhanced Resolution Imaging from Irregular Samples," *IEEE Trans. Geosci. Remote Sens* g, Vol. 39, No. 2, pp. 291-302, 2001.

[4] D. G. Long, P. Hardin, and P. Whiting, "Resolution Enhancement of Spaceborne Scatterometer Data *IEEE Trans. Geosci. Remote Sens*, Vol. 31, No. 3, pp. 700-715, May 1993.

[5] D.G. Long, M.W. Spencer, and E.G. Njoku, "Spatial Resolution and Processing Tradeoffs for HYDROS: Application of Reconstruction and Resolution Enhancement Techniques," *IEEE Trans. Geosci. Remote Sens*, Vol. 43, No. 1, pp. 3-12, 2005.

[6] D.G. Long, and D.L. Daum, "Spatial Resolution Enhancement of SSM/I Data," *IEEE Trans. Geosci. Remote Sens*., Vol. 35, No. 2, pp. 407-417, 1998.

[7] B. Caccin, C. Roberti, P. Russon, and A. Smaldone, "The Backus-Gilbert Method and the Processing of Sampled Data," *IEEE Trans. Signal Proc.*, Vol. 40, pp 2823-2825, 1992.

[8] P. Gilbert, "Iterative Methods for the Three-Dimensional Reconstruction of an Object from Projections," *J. Theor. Bio.* Vol. 36, pp. 105-117, 1972.